# Flow Through Mixed Fibrous Porous Materials

**C. Ross Ethier**
Dept. of Mechanical Engineering, University of Toronto, Toronto, Ontario M5S 1A4, Canada

*Creeping flow through a composite porous material composed of two fiber types has been analyzed for the situation in which the radii of the two fiber populations are highly dissimilar. The composite material has been idealized as a porous matrix that is composed of fine fibers (permeability $K_f$), into which cylindrical inclusions (radius $a_c$) have been embedded, and flow through the resulting system has been modeled by the Debye-Brinkman equation. Two different methods of accounting for the random geometry of a real porous material have been considered: a unit cell approach and replacement of the coarse fibers by a periodic fiber lattice. Model results are in good agreement with each other and reduce in the appropriate limit to well-accepted models for flow in single-component fibrous materials. Plots of net composite permeability as a function of fiber diameter and packing density are presented. In the parameter ranges of interest, viscous effects at the coarse fiber surfaces lead to a significantly lower overall permeability than that predicted by a simple application of Darcy's law.*

## Introduction

Creeping flow through "fibrous porous materials," meaning any network of cylinders (fibers and rods) separated by irregular interstices through which fluid may flow, is of interest in a number of situations. Examples include solvent permeation through polymeric networks (Fessler and Ogston, 1951; Jackson and James, 1982; Ethier, 1986), flow through fibrous filtration devices (see, for example, Kirsch and Stechkina, 1978), and fluid drainage through many bodily tissues (Curry and Michel, 1980; Ethier et al., 1986; Levick, 1987). For such materials it is acceptable to replace somewhat irregular and gradually-curving constitutent fibers by a random array of right circular cylinders (the so-called fiber matrix model). The permeability of the original material can, in principle, then be related to relevant microstructural parameters, namely, the diameter, packing densities, and the orientations of constitutent cylinders. For simple media composed of fibers of uniform radius which are either randomly distributed or placed in periodic arrays, this relationship is provided by several well-known models (Hasimoto, 1959; Happel, 1959; Kuwabara, 1959; Spielman and Goren, 1968) or their extensions (Neale and Masliyah, 1975; Yu and Soong, 1975; Guzy et al., 1983; Sangani and Acrivos, 1982a, b). These models lead to expressions of the general form

$$\frac{K}{a^2}=f(\phi) \tag{1}$$

where $K$ is the material's hydrodynamic permeability, $a$ is the fiber radius, $f(\phi)$ is a model-dependent function, and $\phi$ is the fiber solid fraction, defined as the volume occupied by fibers divided by total volume. The above-mentioned models yield predictions in reasonable agreement with experimental data on flow through monodisperse fibrous materials, at least for low solid fractions (Jackson and James, 1986).

Unfortunately, real fibrous materials can be composed of mixtures of fibers having different diameters, so that the above (monodisperse) models no longer apply. For example, a variety of connective tissue types consist effectively of two fiber populations whose radii differ by a factor of 25 to 100 (Levick, 1987). In these tissues, the volume fractions of the two fiber types are such that the two fiber populations have similar specific surface values, suggesting that both fiber types will be hydrodynamically significant. For such materials, more complete theories taking into account the polydispersity of the fiber population are, therefore, required.

For the special case of materials that are not highly polydisperse, in which fiber radii differ by a factor of two or less, several relationships based either on limited experiments (Kirsch and Fuchs, 1973; Kirsch and Stechkina, 1978) or approximate theories (Ethier, 1983; see also Levick, 1987) have been proposed. These relationships are not valid for highly polydisperse materials. Based on experiments with air flow through highly polydisperse glass fiber filters, Clarenburg and Werner (1965;

see also Werner and Clarenburg, 1965) proposed an empirical relationship for permeability in terms of filter composition. Unfortunately, molecular slip effects were significant in their experiments (Knudson numbers of order one), and thus their empirical relationship is of extremely limited generality; for example, it will not be valid for a permeating fluid other than air. Alternatively, Clarenburg and Schiereck (1968) attempted to extend Clarenburg and Piekaar's (1968) monodisperse fibrous filter theory to multicomponent materials, with poor results. For example, in the appropriate limit their results are not consistent with those of the well-accepted Happel monodisperse model. In short, there is a need for a model describing flow through highly polydisperse fibrous materials, which is independent of empirical experimental input and reduces, in the limit as the solid fraction of one component vanishes, to a well-accepted model for flow through monodisperse materials.

In this article, we formulate such a model by approximating the fine component as a homogeneous porous matrix into which the coarse fibers are embedded. The hydrodynamic effects of both components are then included by using the Debye-Brinkman equation to model the flow. Several different spatial arrangements for the coarse fibers are considered: a doubly periodic square array of coarse fibers and a random array of coarse fibers. The basic model is formulated, and solutions for three possible coarse fiber orientations are presented. Results are compared, and then the approximations made in the theoretical derivations and of the applicability of the results are discussed.

## Model Formulation

We restrict attention to highly-polydisperse, two-component materials which can be idealized as a system of coarse fibers (radius $a_c$ and solid fraction $\phi_c$) embedded in a matrix of finer fibers (radius $a_f$ and solid fraction $\phi_f$), see Figure 1. The disparity in fiber sizes is assumed to be such that the fine matrix appears homogeneous on the length scale of the coarse fibers; this approximation is further considered in the Discussion section. If this holds, we may simply characterize the fine matrix by a permeability $K_f$, which may be calculated, for example, from the Happel single-component theory using fiber radius $a_f$ and local solid fraction $\phi_f/(1-\phi_c)$. Essentially we treat the two-component material as a composite porous material consisting of impermeable (coarse) cylindrical inclusions imbedded in a fine matrix (Figure 2). Implicit in this treatment is spatial averaging of the velocity ($\underline{v}$) and pressure ($p$) fields over a length scale larger than the mean center-to-center spacing within the fine material, but smaller than the coarse fiber radius. Velocities referred to throughout should, therefore, be considered as superficial velocities from the viewpoint of the fine matrix and interstitial velocities from the viewpoint of the coarse matrix.

Hydrodynamically, the coarse fibers have the following effects:

1. They increase the superficial velocity through the fine material due to an "area obstruction" effect.
2. They increase the overall tortuosity of the mixed material.
3. They create velocity gradients within the fine material due to the fact that the no-slip condition must be satisified on the surface of the coarse fibers (Figure 2).

All three effects will tend to decrease the net permeability

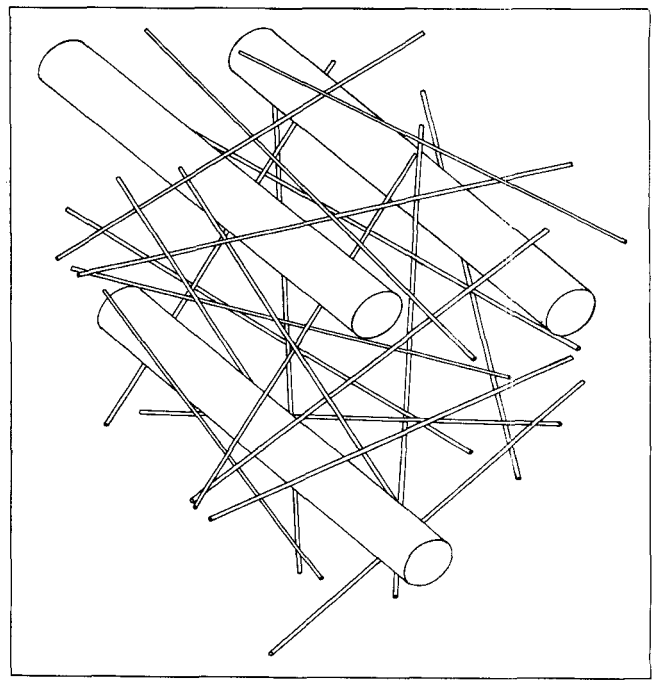

**Figure 1. Idealized view of a two-component, highly-polydisperse, fibrous, porous material.**

Here, the coarse fibers are parallel to one another, but this need not be the case.

of the composite material, $K_{net}$; evidently $K_f$ is an upper bound for $K_{net}$.

To account for velocity gradients within the fine matrix it is necessary to use a higher-order equation than Darcy's law, and we have therefore chosen to model flow through the composite material by the Debye-Brinkman equation:

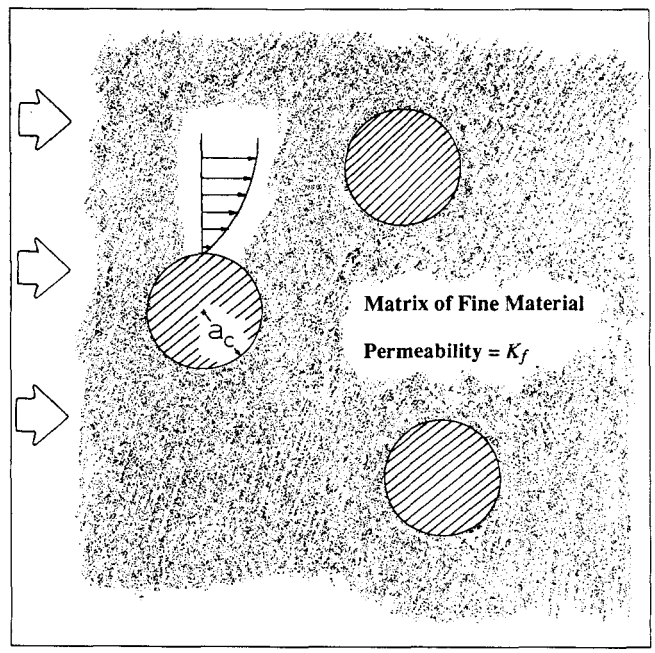


**Figure 2. Idealized view of the postulated hydrodynamically equivalent composite material for cross-flow geometry.**

$$\underline{0} = -\nabla p + \mu' \nabla^2 \underline{v} - \frac{\mu}{K_f} \underline{v} \tag{2}$$

which accounts for the presence of the porous matrix by inclusion of a first-order bulk stress term $\mu/K_f \underline{v}$, while also allowing for the presence of vorticity in $\underline{v}$. In Eq. 2, $\mu$ is the viscosity of the percolating fluid, and $\mu'$ is a viscosity coefficient. There has been some discussion regarding the correct choice of this latter coefficient. Detailed numerical calculations carried out by Larson and Higdon (1986) showed that $\mu'$ could differ from $\mu$ by as much as 25% for $\phi = 0.2$, while Koplik et al. (1983) have shown that $\mu' = \mu$ only in the limit as $\phi$ approaches zero. On the other hand, many authors simply set $\mu' = \mu$ (Neale and Nader, 1974; Adler et al., 1978; Spielman and Goren, 1968; Sano, 1983; Guzy et al., 1983), an approach that has some experimental justification (Matsumoto and Suganuma, 1977). We adopt this latter approach, expecting that this will be a good approximation as long as $\phi_c$ is small, which is typically the case.

If we scale positions, velocities, and stresses by $K_f^{1/2}$, $U_o$, and $\mu U_o K_f^{-1/2}$, then Eq. 2 can be written in dimensionless form as

$$\underline{0} = -\nabla p + \nabla^2 \underline{v} - \underline{v} \tag{2a}$$

to which we append the usual incompressibility requirement, $\nabla \cdot \underline{v} = 0$. In Eq. 2a and all subsequent text, all quantities are dimensionless, unless otherwise noted.

To represent the coarse fiber distribution within a real (random) fibrous material, we have considered several approximate models. In the first approach, the coarse fibers are replaced by a periodic square lattice (Hasimoto, 1959; Sparrow and Loeffler, 1959; Sangani and Acrivos, 1982a,b), having the same solid fraction $\phi_c$ as the original material. Denoting the center-to-center coarse fiber spacing by $2h$ (Figure 3a), the condition

$$h = \frac{a_c}{2}\left[\frac{\pi}{\phi_c}\right]^{1/2} \tag{3}$$

holds. In the second approach, a cylindrical unit cell is constructed around a representative coarse fiber (Happel, 1959; Kuwabara, 1959; Neale and Masliyah, 1975), and the influence of the surrounding fibers is accounted for in an approximate way via boundary conditions at the cell boundary. The cell radius $b_c$ (Figure 3b) is chosen so that the coarse solid fraction within the unit cell equals $\phi_c$,

$$\phi_c = \frac{a_c^2}{b_c^2} \tag{4}$$

It is recognized that both approaches are approximations that neglect statistical variations in interfiber spacing that will occur in real fibrous media. If such variations are not too severe, however, we expect our results will be reasonably accurate. This expectation is based on the success of analogous models for describing flow in monodisperse fibrous materials.

To estimate $K_{net}$ for the composite material we focus attention on a single representative coarse fiber, either in a unit cell or periodic lattice, and solve Eq. 2a for the flow field around this fiber. The mean fluid velocity within the composite material can then be related to the mean pressure gradient, and hence $K_{net}$ can be calculated. In this procedure, it is necessary

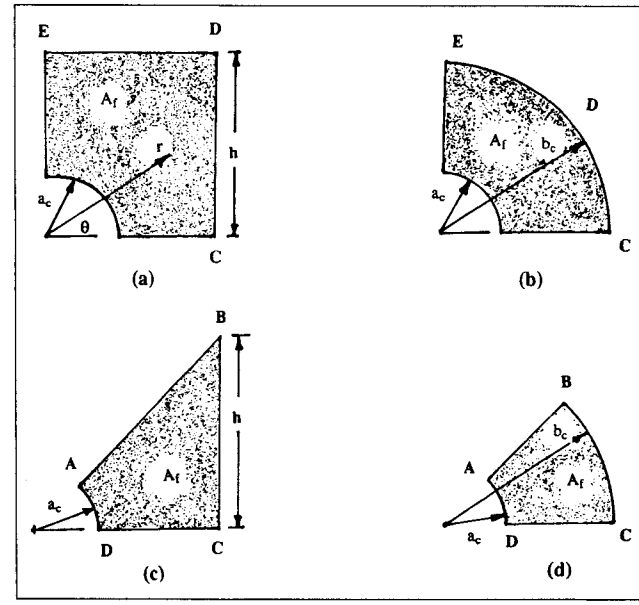


**Figure 3. Definition sketch for: cross-flow, coarse cylinder lattice (3a); cross-flow, unit cell approach (3b), parallel-flow, coarse cylinder lattice (3c); parallel-flow, unit cell approach (3d).**

$A_f$ is the cross-sectional area of the fine matrix. Flow is from right to left.

to consider two geometries: one in which the coarse fiber's axis is perpendicular to the mean flow direction ("cross-flow") and one in which it is parallel ("parallel flow"). The general case of randomly oriented cylindrical inclusions can then be handled by appropriate weighted averaging of the cross-flow and parallel flow cases (Spielman and Goren, 1968). We consider the cross-flow case first.

## Cross Flow

### *Preliminaries*

Following the general approach of Sangani and Acrivos (1982a), we adopt the vorticity-stream function formulation, in which the governing equations become:

$$\nabla^2 \psi = -\omega \tag{5}$$

$$\nabla^2 \omega = \omega \tag{6}$$

For later convenience, define

$$\psi_h = \psi + \omega \tag{7}$$

which allows Eq. 5 to be rewritten as:

$$\nabla^2 \psi_h = 0 \tag{5a}$$

With reference to Figure 3a, symmetry requirements dictate that $\omega = 0$ along $\theta = 0$ and that

$$\frac{\partial \omega}{\partial x} = \frac{\partial \psi}{\partial x} = 0$$

along $\theta = \pi/4$. As well, we set $\psi = 0$ along $\theta = 0$. The solution of Eqs. 5a and 6 satisfying these conditions is

$$\omega = \sum_{n=1}^{\infty} f_n(r) \sin (2n-1)\theta;$$

$$f_n(r) = A_n \frac{I_{2n-1}(r)}{\hat{I}_{2n-1}} + C_n \frac{K_{2n-1}(r)}{\hat{K}_{2n-1}} \quad (8)$$

$$\psi_h = \sum_{n=1}^{\infty} g_n(r) \sin (2n-1)\theta;$$

$$g_n(r) = B_n \left[\frac{r}{a_c}\right]^{2n-1} - D_n \left[\frac{r}{a_c}\right]^{1-2n} \quad (9)$$

in which $I_v$ and $K_v$ are the modified Bessel functions of the first and second kind of order $v$ and the carat indicates that the function is evaluated at $r = a_c$. In the above expressions, $A_n$, $B_n$, $C_n$, and $D_n$ are coefficients determined by the boundary conditions. When the no-slip ($\partial\psi/\partial r = 0$) and no-penetration ($\psi = 0$) conditions are imposed at $r = a_c$, the following constraints on the $A_n$, $B_n$, $C_n$, and $D_n$ are obtained:

$$C_n = y_n A_n - z_n B_n \quad (10a)$$

$$D_n = -(1+y_n)A_n + (1+z_n)B_n \quad (10b)$$

where

$$y_n = \frac{\hat{K}_{2n-1}}{\hat{K}_{2n-2}} \frac{\hat{I}_{2n-2}}{\hat{I}_{2n-1}} \qquad z_n = \frac{\hat{K}_{2n-1}}{\hat{K}_{2n-2}} \frac{2(2n-1)}{a_c} \quad (11)$$

These expressions allow $C_n$ and $D_n$ to be eliminated from Eqs. 8 and 9 to obtain

$$f_n(r) = A_n \left[\frac{I_{2n-1}(r)}{\hat{I}_{2n-1}} + y_n \frac{K_{2n-1}(r)}{\hat{K}_{2n-1}}\right] - B_n z_n \frac{K_{2n-1}(r)}{\hat{K}_{2n-1}} \quad (12)$$

$$g_n(r) = A_n \left[(1+y_n)\left(\frac{r}{a_c}\right)^{1-2n}\right] + B_n \left[\left(\frac{r}{a_c}\right)^{2n-1} - (1+z_n)\left(\frac{r}{a_c}\right)^{1-2n}\right] \quad (13)$$

The determination of $A_n$ and $B_n$ is deferred to the following sections.

The force $F$ (per unit coarse fiber length) exerted by the fluid on the coarse fiber and the surrounding fine matrix has two components: a force $F_s$ generated by the coarse fiber arising from normal and shear stresses at the fiber's surface and a Darcian drag force $F_v$ generated by the fine matrix. The surface force $F_s$ is given by

$$F_s = \int_\gamma [\sigma_{rr} \cos\theta - \sigma_{r\theta} \sin\theta]\, dS \quad (14)$$

where $\sigma_{rr}$ and $\sigma_{r\theta}$ are the normal and shear stresses, and $\gamma$ is the oriented curve $|r| = a_c$. Since $\psi = 0$ and $\sigma_{r\theta} = \omega$ on $\gamma$ we may rewrite Eq. 14 as

$$F_s = -\int_\gamma [p \cos\theta + \psi_h \sin\theta]\, dS \quad (15)$$

Noting that $G(z) = G(x+iy) = p - i\psi_h$ is analytic then gives

$$F_s = -Im \int_\gamma G(z)dz = -2\pi Re\,[\text{Res}\,(G(z))] \quad (16)$$

where Res($G$) denotes the residues of $G(z)$ inside $\gamma$. Since both $p$ and $\psi_h$ have simple poles at $r = 0$, $G(z)$ has a simple pole at $z = 0$, and the surface force is given by

$$F_s = 2\pi a_c D_1 \quad (17)$$

$F_v$ is given by the following integral

$$F_v = 4\int_{A_f} \underline{v} \cdot \hat{x}\, dA \quad (18)$$

where $A_f$ is the area of the fine matrix shown in Figure 3a. Stokes theorem allows Eq. 18 to be written as:

$$F_v = -4\int_{\partial A_f} \psi dx \quad (19)$$

Since $\psi = 0$ on $AB$ and $BC$ we have

$$F_v = -4\int_{CDE} \psi dx \quad (20)$$

To complete the mathematical specification of the problem it is necessary to impose two additional constraints on the flow field on the boundary $CDE$, the exact form of which depends on the microstructure of the porous material, as detailed below.

### *Periodic coarse fiber spacing*

For the case of a doubly periodic square coarse fiber array (Figure 3a), appropriate boundary conditions on $CDE$ are:

$$\text{On } DE\text{: } \omega = 0;\ \psi_h = h \quad (21a)$$

$$\text{On } CD\text{: } \frac{\partial\omega}{\partial x} = \frac{\partial\psi_h}{\partial x} = 0 \quad (21b)$$

These are applied in the manner described by Sangani and Acrivos (1982a). Specifically, the infinite sums in Eqs. 8 and 9 are truncated at $N$ terms, and Eqs. 21a and 21b are applied at $M$ points on each of $DE$ and $CD$ so as to determine coefficients $\{A_n, B_n;\ n = 1, 2, \ldots N\}$ in the least squares sense. For all reported results we used $M = 30$, $N = 15$, and solution insensitivity to $M$, $N$ was carefully verified.

Determination of $A_1$ and $B_1$ allows $D_1$, and thus $F_s$ to be computed from Eqs. 10b and 17. Equation 20 for $F_v$ is simply

$$F_v = 4h^2 \quad (20a)$$

since $dx = 0$ on side $CD$, and $\psi = h$ on $ED$. Darcy's law written

for the composite material can then be used to determine the net permeability of the composite in cross flow $K_{net,cross}$ as:

$$\frac{K_{net,cross}}{K_f} = \frac{4h^2}{F} = \left[1 + \frac{2\phi_c}{a_c} D_1\right]^{-1} \tag{22}$$

where the macroscopic dimensionless pressure gradient has been equated to the force per unit volume, $F/4h^2$.

### *Random coarse fiber spacing*

For the unit cell geometry (Figure 3b), only the $n = 1$ term of the expansions (Eqs. 8 and 9) is required, and thus the only unknowns are $A_1$ and $B_1$. Simplified boundary conditions are to be applied on the cell boundary so as to account in an approximate manner for the influence of the surrounding material. Two such boundary conditions have been considered in the present work: zero shear at $r = b_c$ and velocity matching to an idealized external flow field at $r = b_c$.

*Zero Shear Model.* In this approach, we follow Happel's 1959 development for monodisperse materials and impose a uniform normal velocity and zero tangential shear at the cell boundary. Zero tangential shear requires:

$$2\frac{\partial^2 \psi}{\partial r^2} = -\omega \text{ at } r = b_c \tag{23a}$$

The uniform normal velocity condition is:

$$\psi = -b_c \sin\theta \text{ at } r = b_c \tag{23b}$$

The resulting equations for $A_1$ and $B_1$ are shown in the Appendix; solution of these equations allows $F_s$ to be calculated. In light of Eq. 23b, Eq. 20 for the Darcian force $F_v$ becomes:

$$F_v = \pi b_c^2 \tag{20b}$$

Darcy's law for the composite then gives:

$$\frac{K_{net,cross}}{K_f} = \frac{\pi b_c^2}{F} = \left[1 + \frac{2\phi_c}{a_c} D_1\right]^{-1} \tag{24}$$

*Matching Model.* The second approach we have adopted for the cross-flow problem is motivated by Spielman and Goren (1968), and particularly by Neale and Nader (1974), Neale and Masliyah (1975), and Guzy et al. (1983), in which the flow field at the cell boundary is matched to an idealized flow field in the remainder of the porous material. The flow field in the porous material outside the cell is also described by the Debye-Brinkman equation, with the important distinction that in this external region the permeability appearing in the bulk stress term in Eq. 2 is $K_{net}$, rather than $K_f$. This description of the external flow field is evidently an approximation; once again we refer to the analogous theory for monodisperse materials in which computed results agree well with experimental data (Jackson and James, 1986). This may be due in part to the fact that the flow field close to the cylinder is only weakly dependent on the boundary conditions at the cell boundary so long as these conditions provide a reasonable approximation to reality.

The external problem (outside the unit cell) is formulated as

$$\nabla^2 \psi^o = -\omega^o \tag{25}$$

$$\nabla^2 \omega^o = \beta^2 \omega^o \tag{26}$$

where $\psi^o$ and $\omega^o$ are the stream function and vorticity outside the unit cell, and

$$\beta = \left[\frac{K_f}{K_{net}}\right]^{1/2} \tag{27}$$

Defining $\psi_h^o = \psi^o + \beta^{-2}\omega^o$ allows Eq. 25 to be replaced by

$$\nabla^2 \psi_h^o = 0 \tag{25a}$$

The external velocity field is uniform far from the test fiber, corresponding to boundary conditions

$$\omega^o \to 0 \qquad \text{as } r \to \infty \tag{28a}$$

$$\psi^o \to r\sin\theta \quad \text{as } r \to \infty \tag{28b}$$

The solution of Eqs. 25a and 26 satisfying Eq. 28 in the unit cell geometry is

$$\omega^o = E_1 \beta^2 \frac{K_1(r\beta)}{K_1(b_c\beta)} \sin\theta \tag{29}$$

$$\psi_h^o = \left[r + F_1 \frac{b_c}{r}\right] \sin\theta \tag{30}$$

where $E_1$ and $F_1$ are constants. Matching of tangential and normal velocities and stresses at the cell boundary then allows $A_1$, $B_1$, $E_1$, and $F_1$ to be expressed in terms of the parameter $\beta$ (see the Appendix). (See Ethier and Kamm, 1989, for a discussion of shear stress matching using the Debye-Brinkman equation.)

It remains to calculate the force on the material within the unit cell. Since $\psi = \psi^o$ on *CDE*, Eq. 20 becomes:

$$F_v = \pi b_c^2 \left[1 + \frac{F_1}{b_c} - \frac{E_1}{b_c}\right] \tag{20c}$$

Thus, Darcy's law for the composite material may be written as:

$$\beta^2 = 1 + \frac{F_1}{b_c} - \frac{E_1}{b_c} + \frac{2\phi_c}{a_c} D_1 \tag{31}$$

Since $D_1$, $E_1$, and $F_1$ are functions of $\beta$, this is a transcendental equation for $\beta$ in terms of $a_c$ and $b_c$. It was solved numerically using Newton linearization to give the following results.

## Parallel Flow

### *Preliminaries*

For the parallel flow case it is most convenient to work in primitive variables, employing a cylindrical coordinate system

with the $\hat{z}$ vector coincident with the fiber axis and the flow direction (Figures 3c and 3d). In this case $dp/dz$ is a constant, and Eq. 2a can be rewritten as

$$\nabla^2 \tilde{v} = \tilde{v} \tag{32}$$

where

$$\tilde{v} = \frac{v_z}{-dp/dz} - 1 \tag{33}$$

In light of the symmetry requirements $\partial\tilde{v}/\partial\theta = 0$ along $\theta = 0$ and $\theta = \pi/4$, the solution of Eq. 32 is

$$\tilde{v} = \sum_{n=1}^{\infty} h_n(r) \cos 4n\,\theta;\ h_n(r) = G_n \frac{I_{4n}(r)}{\hat{I}_{4n}} - H_n \frac{K_{4n}(r)}{\hat{K}_{4n}} \tag{34}$$

where $G_n$ and $H_n$ are constants. Imposing no-slip on the coarse cylinder's surface gives $G_n = H_n$ for $n \geq 1$ and $H_0 = G_0 + 1$, so that $\tilde{v}$ is

$$\tilde{v} = -\frac{K_0(r)}{\hat{K}_0} + \sum_{n=0}^{\infty} G_n \cos 4n\theta \left[ \frac{I_{4n}(r)}{\hat{I}_{4n}} - \frac{K_{4n}(r)}{\hat{K}_{4n}} \right] \tag{35}$$

Specification of the coefficients $G_n$ is deferred to the following sections.

The dimensionless flow rate within the area $A_f$ shown in Figure 3c may be expressed as:

$$\frac{Q}{-dp/dz} = \int_{A_f} (1 + \tilde{v})\, dA \tag{36}$$

Use of Eq. 32 and Green's theorem gives

$$\frac{Q}{-dp/dz} = A_f + \int_{\partial A_f} \frac{\partial \hat{v}}{\partial n}\, dS \tag{37}$$

where $n$ is the normal to the boundary $A_f$. Darcy's law for the composite then becomes

$$\frac{K_{\text{net,parallel}}}{K_f} = \frac{Q}{-dp/dz\,(A_f + \pi a_c^2/8)} = 1 - \phi_c + \frac{8\phi_c}{\pi a_c^2} \int_{\partial A_f} \frac{\partial \tilde{v}}{\partial n}\, dS \tag{38}$$

We now consider several different coarse fiber arrangements.

### *Periodic coarse array*

By analogy with the cross-flow case, the summation in Eq. 35 is truncated at the $N$th term, and the coefficients $\{G_n;\ n = 0 \ldots N\}$ are determined from the boundary condition:

$$\frac{\partial \tilde{v}}{\partial x} = 0 \text{ on } BC \tag{39}$$

Once again Eq. 39 was applied at $M$ points along $BC$ and the $G_n$ were determined by least squares. Results presented below are for $M = 30$, $N = 15$.

To evaluate $Q$, note that $\partial\tilde{v}/\partial n$ vanishes on $AB$, $BC$, and $CD$. As well, only the $n = 0$ term in Eq. 34 contributes to the integral in Eq. 38, so that Darcy's law becomes

$$\frac{K_{\text{net,parallel}}}{K_f} = 1 - \phi_c - \frac{2\phi_c}{a_c} \left[ \frac{\hat{K}_1}{\hat{K}_0} (1 + G_0) + \frac{\hat{I}_1}{\hat{I}_0} G_0 \right] \tag{40}$$

### *Random coarse fiber spacing*

We once again consider the unit cell geometry (Figure 3d), in which case only the $n = 0$ term in Eq. 35 is required. As in the cross-flow problem, two conditions on the cell boundary are considered: zero shear or matching to an idealized external flow field.

*Zero Shear Model.* Again, by analogy with Happel's 1959 development for monodisperse materials, we require that the shear stress vanish on the cell boundary,

$$\sigma_{rz} = \frac{dv_z}{dr} = 0 \quad \text{at } r = b \tag{41}$$

$G_0$ is then trivially given as:

$$G_0 = \frac{-1}{1 + \dfrac{\hat{K}_0}{K_1(b_c)} \dfrac{I_1(b_c)}{\hat{I}_0}} \tag{42}$$

Since $\partial\tilde{v}/\partial n$ on $BC$, $K_{\text{net,parallel}}/K_f$ is once again given by Eq. 40.

*Matching Model.* The flow field within the cell is matched to an idealized external flow field calculated by the Debye-Brinkman equation, as was done for the cross-flow problem. The dimensionless form of the Debye-Brinkman equation which applies outside the cell is

$$0 = -\frac{dp}{dz} + \nabla^2 v_z - \beta^2 v_z \tag{43}$$

where $dp/dz$ within the cell matches $dp/dz$ outside the cell. Subject to the requirement that $v_z$ be bounded at infinity, a solution of Eq. 43 is

$$v_z = -\frac{1}{\beta^2} \frac{dp}{dz} \left[ 1 + L_0 \frac{K_0(r\beta)}{K_0(b_c\beta)} \right] \tag{44}$$

where $L_0$ is a constant. Matching $v_z$ and $\sigma_{rz} = dv_z/dr$ at the cell boundary determines $G_0$ and $L_0$ (see the Appendix). Darcy's law for the composite material (Eq. 38) becomes a transcendental equation for the ratio $\beta^2 = K_{\text{net, parallel}}/K_f$

$$\frac{1}{\beta^2} = 1 - \phi_c - \frac{2\phi_c}{a_c} \left[ \frac{\hat{K}_1}{\hat{K}_0} (1 + G_0) + \frac{\hat{I}_1}{\hat{I}_0} G_0 \right] - \frac{2\phi_c b_c}{a_c^2} \frac{L_0}{\beta^2} \frac{K_1(b_c\beta)}{K_0(b_c\beta)} \tag{45}$$

Numerical solution of Eq. 45 for given $a_c$ and $b_c$ allows $K_{\text{net,parallel}}$ to be determined.

## Random Orientation

For composite materials, in which the coarse fibers are randomly oriented, the linearity of the problem can be exploited to give the net permeability in terms of a weighted sum of $K_{\text{net,cross}}$ and $K_{\text{net,parallel}}$ (Spielman and Goren, 1968). (By randomly oriented, we mean the case in which the probability density function for the angle $\alpha$ between the coarse fibers and the superficial velocity vector within the composite is $\sin \alpha d\alpha$.) Thus,

$$\frac{1}{K_{\text{net, random}}} = \frac{2/3}{K_{\text{net,cross}}} + \frac{1/3}{K_{\text{net,parallel}}} \tag{46}$$

It is, of course, nonsensical to speak about a randomly oriented set of coarse cylinders in the context of the periodic lattice model, and thus the lattice approach breaks down in this case. However, as an approximation to a real material, the periodic coarse lattice results for the parallel and cross-flow geometries can still be combined through Eq. 46.

For the matching model, the above equation is not self-consistent, and a slightly different approach is used, as follows. The cross-flow and parallel-flow models are solved with the external medium having an unknown permeability $K_{\text{net,random}}$, yielding expressions for $K_{\text{net,cross}}$ and $K_{\text{net,parallel}}$ as functions of $K_{\text{net,random}}$. $K_{\text{net,cross}}$ and $K_{\text{net,parallel}}$ are then substituted into Eq. 46 to yield a single transcendental equation for $K_{\text{net,random}}$. (In practice, results obtained with this approach are almost identical to those resulting from direct use of Eq. 46.)

## Results

Considering the cross-flow case, initially we plot in Figure 4 the predictions of the unit cell zero shear model for $K_{\text{net,cross}}/a_c^2$ as a function of $\phi_c$ for various values of $K_f/a_c^2$, which provides a rough estimate of the relative hydrodynamic importance of the fine matrix as compared to the coarse fibers. This can be seen most readily by noting that the Debye-Brinkman equation predicts the existence of a velocity transition layer of thickness $O(K_f^{1/2})$ next to boundaries on which the no-slip condition is applied. The ratio $K_f^{1/2}/a_c$, therefore, is the thickness of this layer compared to the coarse fiber radius. When $K_f/a_c^2 \ll 1$, the composite's net permeability is governed primarily by the fine material, and thus $K_f$ is a good estimate for $K_{\text{net,cross}}$. On the other hand, when $K_f/a_c^2 \gg 1$, the effects of the fine material become insignificant and the coarse fibers provide the main resistance to flow, and we expect to recover the results of theories for flow through a monodisperse fibrous material having fiber radius $a_c$ and solid fraction $\phi_c$.

This limiting behavior is confirmed by Figure 4. Note that as $K_f/a_c^2 \to \infty$, our model results approach those of the Happel (1959) single-component model. Although not shown, similar limiting behavior is noted as $K_f/a_c^2 \to \infty$ for the unit cell matching model, where the results approach those of Guzy et al. (1983). A second limiting case is obtained when $K_f/a_c^2 \to 0$. It can be shown that both the zero shear model and the matching model (for small $\phi_c$) give

$$\frac{K_{\text{net,cross}}}{K_f} \to \frac{1-\phi_c}{1+\phi_c} \text{ as } K_f/a_c^2 \to 0 \tag{47}$$

as previously predicted by Paleszewski (1983). This limit corresponds to the situation in which the coarse fibers act to increase the tortuosity and the superficial velocity within the fine matrix, but exert a negligible hydrodynamic effect via the no-slip condition. The $1-\phi_c$ term in the numerator of Eq. 47 represents an "area obstruction" effect by the coarse fibers, leading to an increased superficial velocity within the fine material. The $(1+\phi_c)^{-1}$ term in Eq. 47 accounts for the increased tortuosity introduced by the coarse fibers.

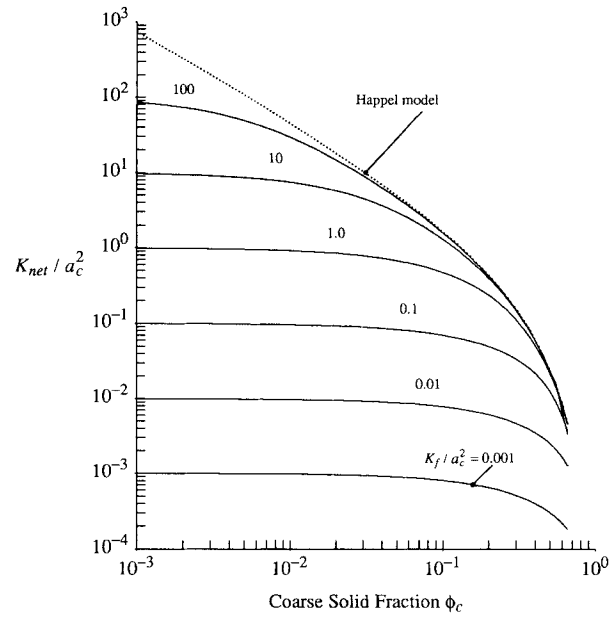


**Figure 4. Dimensionless net permeability, $K_{net}/a_c^2$ vs. coarse solid fraction $\phi_c$ for various values of the ratio $K_f/a_c^2$ for the cross-flow geometry.**

The results are predicted by the zero shear unit cell model (Eqs. 24 and A8). Also shown are the results of the monodisperse Happel model (dotted line).

The results of all the cross-flow models are compared in Figure 5, where $K_{\text{net,cross}}/K_f$ is shown as a function of $\phi_c$ and $K_f/a_c^2$. The three models are seen to be in good general agreement with one another, with best agreement between the periodic lattice model and the unit cell matching model. Although results are presented for $\phi_c$ as large as 0.65, the present models are expected to be most accurate for small $\phi_c$, i.e., $0 \le \phi_c \le 0.3$. In this range of $\phi_c$, differences between the models are of the order of 15%, with a worst-case difference of approximately 35% at $K_f/a_c^2 = 1$, $\phi_c = 0.3$.

Figures 6 and 7 show results for the parallel and random coarse fiber orientations. For the parallel flow case, the following limiting form is obtained:

$$\frac{K_{\text{net,parallel}}}{K_f} \to 1-\phi_c \text{ as } \frac{K_f}{a_c^2} \to 0 \tag{48}$$

Comparing this result with Eq. 47 shows that the $(1+\phi_c)^{-1}$ term (representing an increase in tortuosity due to the coarse fibers) is absent, as one would expect for the parallel geometry. The corresponding equation for the random fiber orientation is:

$$\frac{K_{\text{net,random}}}{K_f} \to \frac{1-\phi_c}{1+2/3\phi_c} \text{ as } \frac{K_f}{a_c^2} \to 0 \tag{49}$$

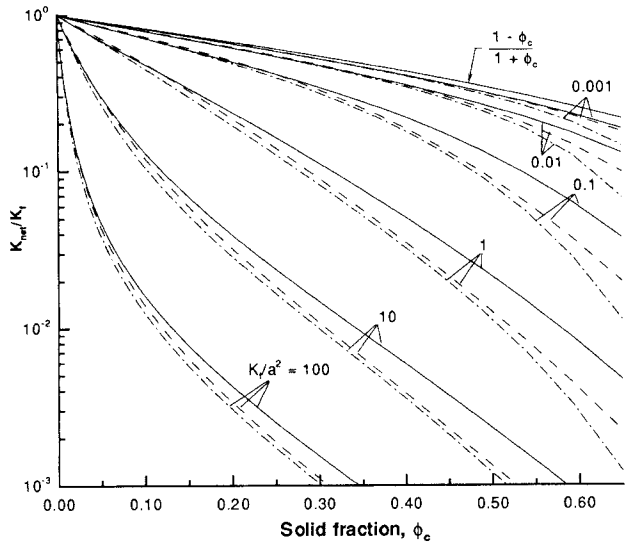


**Figure 5. Dimensionless net permeability, $K_{net}/K_f$ vs. coarse solid fraction $\phi_c$ for various values of the ratio $K_f/a_c^2$ in the cross-flow geometry.**

——, unit cell zero shear model; ----, unit cell matching model; -·-·-, periodic lattice model. Also shown (——) is the limiting form predicted as $K_f/a_c^2 \to 0$.

The general features of the parallel and random orientation cases are quite similar to those of the cross-flow case.

## Discussion

The models presented above give $K_{net}$ as a function of $a_c$, $K_f$ and $\phi_c$ for the cross-flow, parallel-flow, and random orientations of the coarse fibers within a two-component fibrous material. As well, for each orientation a periodic lattice arrangement and a random arrangement for the coarse fibers have been considered. Ideally, we would validate the models

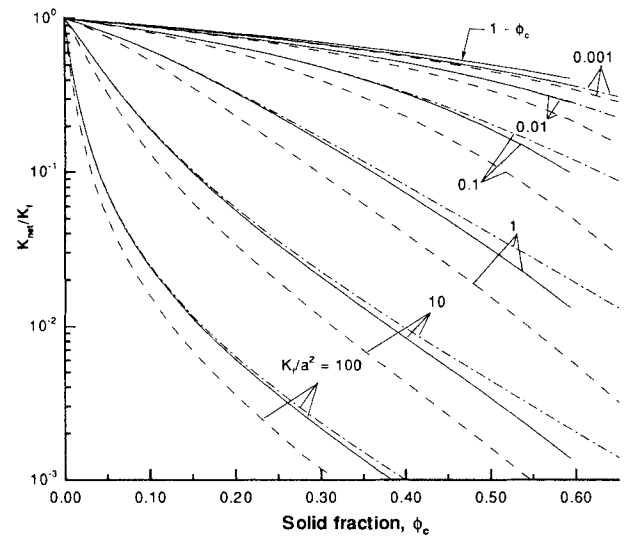


**Figure 6. Dimensionless net permeability, $K_{net}/K_f$ vs. coarse solid fraction $\phi_c$ for various values of the ratio $K_f/a_c^2$ for the parallel geometry.**

Legend as for Figure 5.

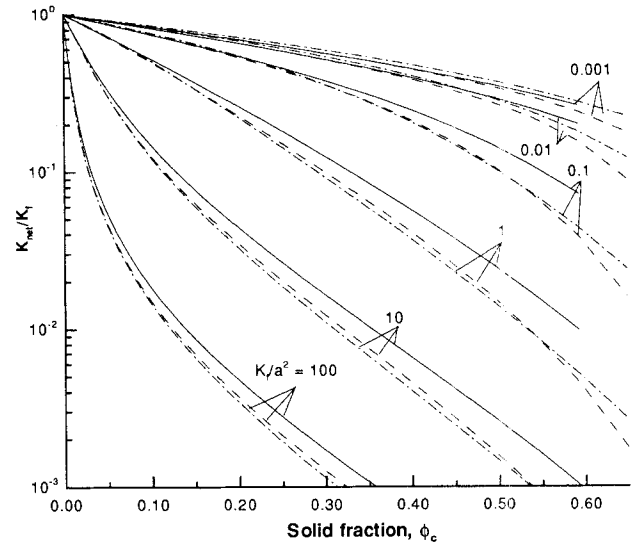


**Figure 7. Dimensionless net permeability, $K_{net}/K_f$ vs. coarse solid fraction $\phi_c$ for various values of the ratio $K_f/a_c^2$ for the random fiber geometry.**

Legend as for Figure 5.

by comparing these results with a reliable body of experimental data. However, as previously noted, we are unaware of any experimental studies on flow through, well-controlled, two-component, fibrous materials appropriate for the present study. We, therefore, resort to a critical examination of the results and assumptions underlying the models.

In comparing results from the different models, we recognize that each model approximates the geometry and flow field within a real fibrous material in a different manner. Nonetheless, typical differences in the permeability predictions of the three models are of the order of 15–20% for the cross-flow and random orientation geometries, at least in the range $0 \le \phi_c \le 0.3$. (Slightly more variation is seen for parallel flow.) This degree of variability is typically seen in permeability measurements on real random materials (e.g., Jackson and James, 1986), and thus the results of the above models in the range $0 \le \phi_c \le 0.3$ may be considered equivalent for most engineering purposes. The preferred model, therefore, is the unit cell zero shear approach, due to its relative computational simplicity. This consistency among model predictions enhances confidence in the results of this study and suggests that our treatment of coarse fiber geometric effects are reasonable, in accordance with experience with monodisperse fibrous media. (Of course, for a material containing a periodic square lattice of coarse cylinders, the periodic lattice model is "exact," subject to the following discussion.)

An assumption common to all of the models is the replacement of the fine cylinders by a matrix that is homogeneous on the length scale $a_c$ and subsequent treatment of this fine matrix by a bulk stress term in the Debye-Brinkman equation. We expect that treatment of the fine cylinders via a homogeneous bulk stress term in the Debye-Brinkman equation will be acceptable, if the volume fraction of fine fibers is small and if the fine material can be considered as homogeneous and isotropic on the length scale of the coarse fibers. The former condition will be satisfied for most fibrous materials of interest and thus is not restrictive. A necessary condition for homo-

geneity is that the mean distance between fine fibers be much less than the coarse fiber radius,

$$\phi_f \left[\frac{a_c}{a_f}\right]^2 \gg 1 \tag{50}$$

In the present study, we are most interested in materials for which $K_f/a_c^2$ is of order unity (see below). For such materials and for typical $\phi_f$ values (order $10^{-2}$ to $10^{-3}$), the left side of Eq. 50 is of order one. Hence, in this case, the homogeneity requirement Eq. 50 will not be strictly satisfied. However, we suggest that the present results will still be valid for three reasons.

1. Numerical modeling by Larson and Higdon (1986) suggests that the Debye-Brinkman approach is acceptable even when this homogeneity requirement is satisfied only approximately.

2. It must be remembered that a fluid particle will sample many "unit cells," as it passes through a real fibrous material. Even though the fine fibers within any individual cell may not be homogeneous, the effect of the fine fibers, when ensemble averaged over all "unit cells" encountered by the fluid particle, can be approximated by a homogeneous material. Of course, the flow field around any given coarse fiber may differ from the average computed here, but in the present work we are concerned only with overall pressure drop, rather than the flow around a given coarse fiber.

3. The above models give the correct behavior in the limits, as $K_f/a_c^2$ approaches zero and infinity due to the fact that the Debye-Brinkman equation reduces to Darcy's law or the Stokes equations in these limits. One could, therefore, view the present work as an asymptotically correct theory that bridges the gap between these limits in a rational manner.

The present models will be most useful for materials in which $K_f/a_c^2$ is O(1). For very large values of this ratio, the permeability is estimated more easily by single-component theory; for very small values flow through the fine matrix is more easily described by Darcy's law (Eqs. 47 and 48). Note that for $\phi_c = 0.3$ and $K_f/a_c^2 = 1$, a naive application of the Darcian result (Eq. 47) will lead to an approximate tenfold overestimate for net permeability in the cross-flow case. This emphasizes the need to account for viscous effects at the coarse fiber surfaces in such a case.

## Acknowledgment

The author would like to thank Dr. Mark Johnson for many valuable discussions and suggestions. This work was supported by Canadian NSERC Grant A2191.

## Notation

$a$ = fiber radius
$A_f$ = area of fine material, Figure 3
$A_n, B_n, C_n, D_n$ = coefficients in expansions (Eqs. 8 and 9)
$E_1, F_1$ = constants in Eqs. 29 and 30
$F_s$ = drag force generated by stresses at the coarse cylinder surface, per unit coarse cylinder length
$F_v$ = drag force generated by the fine matrix, per unit coarse cylinder length
$G(z)$ = $p - i\psi_h$
$G_n, H_n$ = constants in expansion (Eq. 34)
$h$ = half center-to-center fiber spacing in periodic lattice
$I_v, K_v$ = modified Bessel functions of the first and second kind of order $v$
$K$ = permeability
$K_{net}$ = net composite permeability
$L_0$ = constant (Eq. 44)
$Q$ = flow rate
$U_0$ = reference velocity
$v_z$ = velocity in $z$ direction
$\tilde{v}$ = see Eq. 33
$y_n, z_n$ = see Eq. 11

### *Greek letters*

$\beta$ = see Eq. 27
$\gamma$ = oriented curve $|r| = a_c$
$\mu, \mu'$ = fluid viscosity, viscosity coefficient appearing in Debye-Brinkman equation
$\phi$ = fiber solid fraction
$\psi$ = stream function
$\psi_h$ = function defined by Eq. 7
$\psi_h^o$ = function defined by $\psi_h^o = \psi^o + \beta^{-2}\omega^o$
$\sigma$ = fluid stress tensor
$\omega$ = vorticity

### *Subscripts*

$f$ = fine component
$c$ = coarse component

### *Superscripts*

$o$ = quantity defined outside the unit cell in matching model
$\hat{}$ = function evaluated at $r = a_c$

## Literature Cited

Adler, P. M., P. M. Mills, and D. C. Quemada, "Application of a Self-Consistent Model to the Permeability of a Fixed Swarm of Permeable Spheres," *AICHE J.*, **24**, 354 (1978).

Clarenburg, L. A., and H. W. Piekaar, "Aerosol Filters: I. Theory of the Pressure Drop Across Single Component Glass Fibre Filters," *Chem. Eng. Sci.*, **23**, 765 (1968).

Clarenburg, L. A., and F. C. Schiereck, "Aerosol Filters: II. Theory of the Pressure Drop Across Multicomponent Glass Fibre Filters," *Chem. Eng. Sci.*, **23**, 773 (1968).

Clarenburg, L. A., and R. M. Werner, "Aerosol Filters: Pressure Drop Across Multicomponent Glass Fibre Filters," *Ind. and Eng. Chem. Proc. Des. and Dev.*, **4**, 293 (1965).

Curry, F. E., and C. C. Michel, "A Fiber Matrix Model of Capillary Permeability," *Microvasc Res.*, **20**, 96 (1980).

Ethier, C. R., "Hydrodynamics of Flow Through Gels with Applications to the Eye," S. M. Thesis, M.I.T., Boston, (1983).

Ethier, C. R., "The Hydrodynamic Resistance of Hyaluronic Acid: Estimates From Sedimentation Studies," *Biorheology*, **23**, 99 (1986).

Ethier, C. R., R. D. Kamm, B. A. Palaszewski, M. C. Johnson, and T. M. Richardson, "Calculations of Flow Resistance in the Juxtacanalicular Meshwork," *Invest. Ophthal. Vis. Sci.*, **27**, 1741, (1986).

Ethier, C. R., and R. D. Kamm, "Flow Through Partially Gel-Filled Channels, *PCH J.*, **11**, 219 (1989).

Fessler, J. H., and A. G. Ogston, "Sarcosine Polymers," *Trans. Farad. Soc.*, **47**, 667 (1951).

Guzy, C. J., E. J. Bonano, E. J. Davis, "The Analysis of Flow and Colloidal Particle Retention in Fibrous Porous Media," *J. Coll. Int. Sci.*, **95**, 523 (1983).

Happel, J., "Viscous Flow Relative to Arrays of Cylinders," *AIChE J.*, **5**, 174 (1959).

Hasimoto, H., "On the Periodic Fundamental Solutions of the Stokes Equations and Their Application to Flow Past a Cubic Array of Spheres," *J. Fluid Mech.*, **5**, 317 (1959).

Jackson, G. W., and D. F. James, "The Hydrodynamic Resistance of Hyaluronic Acid and Its Contribution to Tissue Permeability," *Biorheology*, **19**, 317 (1982).

Jackson, G. W., and D. F. James, "The Permeability of Fibrous Porous Media," *Can. J. Chem. Eng.*, **64**, 364, (1986).
Kirsch, A. A., and N. A. Fuks, "Pressure Drop and Aerosol Deposition in a Polydisperse Fan-Model Filter," *Colloid J.*, **35**, 906 (1973).
Kirsch, A. A., and I. B. Stechkina, "The Theory of Aerosol Filtration with Fibrous Filters," *Fundamentals of Aerosol Science*, Shaw, D. T., ed., Wiley (1978).
Koplik, J., H. Levine, and A. Zee, "Viscosity Renormalization in the Brinkman Equation," *Phys. Fluids*, **26**, 2864 (1983).
Kuwabara, S., "The Force Experienced by Randomly Distributed Parallel Circular Cylinders or Spheres in a Viscous Flow at Small Reynolds Numbers," *J. Phys. Soc. Japan*, **14**, 527 (1959).
Larson, R. E., and J. J. L. Higdon, "Microscopic Flow Near the Surface of Two-Dimensional Porous Media: 1. Axial Flow," *J. Fluid Mech.*, **166**, 449 (1986).
Levick, J. R., "Flow Through Interstitium and Other Fibrous Matrices," *Quart. J. Exp. Physiol.*, **72**, 409 (1987).
Matsumoto, K., and A. Suganuma, "Settling Velocity of a Permeable Model Floc," *Chem. Eng. Sci.*, **32**, 445 (1977).
Neale, G., and J. H. Masliyah, "Flow Perpendicular to Mats of Randomly Arranged Cylindrical Fibers," *AIChE J.*, **21**, 805 (1975).
Neale, G. H., and W. K. Nader, "Prediction of Transport Processes Within Porous Media: Creeping Flow Relative to a Fixed Swarm of Spherical Particles," *AIChE J.*, **20**, 530 (1974).
Palaszewski, B., "Analytical Studies of Flow Through a Porous Medium with Applications to the Trabecular Meshwork of the Eye," S. M. Thesis, M.I.T., Boston (1983).
Sangani, A. S., and A. Acrivos, "Slow Flow Past Periodic Arrays of Cylinders with Application to Heat Transfer," *Int. J. Multiphase Flow*, **8**, 193 (1982a).
Sangani, A. S., and A. Acrivos, "Flow Through a Periodic Array of Spheres," *Int. J. Multiphase Flow*, **8**, 343 (1982b).
Sano, O., "Viscous Flow Past a Cylindrical Hole Bored Inside a Porous Media—With Application to Measurement of the Velocity of Subterranean Water by the Single Boring Method," *Nagare*, in Japanese **2**, 252 (1983).
Sparrow, E. M., and A. L. Loeffler, "Longitudinal Laminar Flow between Cylinders Arranged in Regular Array," *AIChE J.*, **5**, 325 (1959).
Spielman, L., and S. L. Goren, "Model for Predicting Pressure Drop and Filtration Efficiency in Fibrous Media," *Env. Sci. Tech.*, **2**, 279 (1968).
Werner, R. M., and L. A. Clarenburg, "Aerosol Filters—Pressure Drop Across Single-Component Glass Fiber Filters," *Ind. and Eng. Chem. Proc. Des. and Dev.*, **4**, 288 (1965).
Yu, C. P., and T. T. Soong, "A Random Cell Model for Pressure Drop Prediction in Fibrous Filters," *Trans. ASME J. Appl. Mech.*, **E97**, 301 (1975).

## Appendix

Reproduced below are the constraints used to determine the coefficients $A_n$ and $B_n$ for the unit cell approach in the following cases: (1) cross-flow, zero shear; (2) cross-flow, external-flow field matching; and (3) parallel-flow, external-flow field matching.

### *Cross-flow, zero shear*

To simplify notation, we make the following definitions:

$$P_n = \frac{I_{2n-1}(r)}{\hat{I}_{2n-1}} + y_n \frac{K_{2n-1}(r)}{\hat{K}_{2n-1}} \tag{A1}$$

$$Q_n = z_n \frac{K_{2n-1}(r)}{\hat{K}_{2n-1}} \tag{A2}$$

$$R_n = \frac{I_{2n-2}(r)}{\hat{I}_{2n-1}} - y_n \frac{K_{2n-2}(r)}{\hat{K}_{2n-1}} \tag{A3}$$

$$S_n = -z_n \frac{K_{2n-2}(r)}{\hat{K}_{2n-1}} \tag{A4}$$

$$T_n = (1+y_n)\left(\frac{r}{a_c}\right)^{1-2n} \tag{A5}$$

$$U_n = \left(\frac{r}{a_c}\right)^{2n-1} - (1+z_n)\left(\frac{r}{a_c}\right)^{1-2n} \tag{A6}$$

$$V_n = \left(\frac{r}{a_c}\right)^{2n-1} + (1+z_n)\left(\frac{r}{a_c}\right)^{1-2n} \tag{A7}$$

The constraints on $A_1$ and $B_1$ can then be written as:

$$\begin{bmatrix} P_1 - T_1 & -Q_1 - U_1 \\ \frac{b_c^2}{2} P_1 - b_c R_1 & V_1 + U_1 + b_c S_1 - \frac{b_c^2}{2} Q_1 \end{bmatrix} \begin{bmatrix} A_1 \\ B_1 \end{bmatrix} = \begin{bmatrix} b_c \\ -b_c \end{bmatrix} \tag{A8}$$

### *Cross-flow matching to external-flow field*

Matching velocities and stresses is equivalent to matching $\psi$, $\partial\psi/\partial r$ and $\omega$ between inner and outer solutions, plus $\partial\psi_h/\partial r = \beta^2\,\partial\psi_h^o/\partial r$. The resulting constraints on $A_1$, $B_1$, $E_1$, and $F_1$ are:

$$\begin{bmatrix} T_1 - P_1 & Q_1 + U_1 & 1 & -1 \\ -R_1 b_c & V_1 + U_1 + b_c S_1 & -b_c\beta \frac{K_0(b_c\beta)}{K_1(b_c\beta)} & 0 \\ P_1 & -Q_1 & -\beta^2 & 0 \\ -T_1 & V_1 & 0 & \beta^2 \end{bmatrix} \begin{bmatrix} A_1 \\ B_1 \\ E_1 \\ F_1 \end{bmatrix} = \begin{bmatrix} b_c \\ 2b_c \\ 0 \\ b_c\beta^2 \end{bmatrix} \tag{A9}$$

This is solved simultaneously with Eq. 31 to determine $\beta$.

### *Parallel flow matching to external-flow field*

The constraints on $G_0$ and $L_0$ are:

$$\begin{bmatrix} \frac{I_0(b_c)}{\hat{I}_0} - \frac{K_0(b_c)}{\hat{K}_0} & -\frac{1}{\beta^2} \\ \frac{I_1(b_c)}{\hat{I}_0} + \frac{K_1(b_c)}{\hat{K}_0}\,\frac{1}{\beta^2}\,\frac{K_1(b_c\beta)}{K_0(b_c\beta)} & \end{bmatrix} \begin{bmatrix} G_0 \\ L_0 \end{bmatrix} = \begin{bmatrix} \frac{1}{\beta^2} + \frac{K_0(b_c)}{\hat{K}_0} - 1 \\ -\frac{K_1(b_c)}{\hat{K}_0} \end{bmatrix} \tag{A10}$$

This is solved simultaneously with Eq. 45 to determine $\beta$.

*Manuscript received Feb. 21, 1991, and revision received July 8, 1991.*